

Photoluminescence study of localization effects induced by the fluctuating random alloy potential in indirect band-gap $\text{GaAs}_{1-x}\text{P}_x$

M. Oueslati and M. Zouaghi

Laboratoire de Spectroscopie Moléculaire, Département de Physique, Faculté des Sciences de Tunis, Tunis, Tunisia

M. E. Pistol, L. Samuelson, and H. G. Grimmeiss

Department of Solid State Physics, University of Lund, Box 118, S-221 00 Lund, Sweden

M. Balkanski

Laboratoire de Physique des Solides, Université Pierre et Marie Curie, 4 place Jussieu, 75230 Paris Cedex 05, France

(Received 23 April 1985)

In the recombination spectra of indirect-band-gap alloys of $\text{GaAs}_{1-x}\text{P}_x$, a peculiar and asymmetric luminescence band, M_0^x , has previously been reported to be due to the fluctuating alloy potential. Detailed experiments are reported here on $\text{GaAs}_{1-x}\text{P}_x$ samples which exhibit exceptionally strong M_0^x luminescence. The properties and line shape of M_0^x have been studied as a function of the sample composition, excitation power densities, and decay times. It is concluded that recombining electron-hole pairs are trapped by the fluctuations of the band edges which form exponential tails in the gap and that the charge carriers are subject to localization below a mobility edge. Calculations performed using this model are able to explain most of the observed behavior of the M_0^x emission band.

I. INTRODUCTION

The composition disorder in III-V semiconductor compound alloys induces different effects observable by luminescence.¹⁻⁵ On one hand, the impurity bound-exciton lines are inhomogeneously broadened; on the other hand, levels of excitons bound to nitrogen impurities in $\text{GaAs}_{1-x}\text{P}_x$ become lower than donor bound-exciton levels with decreasing composition. The large- k components of the fluctuating potential break the k -selection rules,^{6,7} making the zero-phonon transition allowed in indirect band-gap compounds. The random potential induces localized states which give rise to a luminescence band (M_0^x) with unusual properties appearing from 7 to 12 meV below the free exciton. This band has been interpreted either as the recombination of a localized exciton^{8,9} (i.e., the electron and hole having the same origin in space) or as the recombination of a localized electron and a localized hole trapped in different potential wells.¹⁰ The lifetime of the M_0^x luminescence band is very long (5–100 μs) and strongly nonexponential. Such recombination of localized electron-hole pairs has been reported in a number of alloys under particular experimental conditions,⁷⁻¹¹ namely, low-temperature and low-excitation power densities. In this paper, we present experimental results on $\text{GaAs}_{1-x}\text{P}_x$. We have studied the evolution of luminescence spectra with temperature, excitation power, time, and composition x in order to obtain a better characterization of these states. Dye-laser experiments have been used to study resonant luminescence excitation and to measure the luminescence line shape, revealing an exponentially varying density of states in the band-gap.

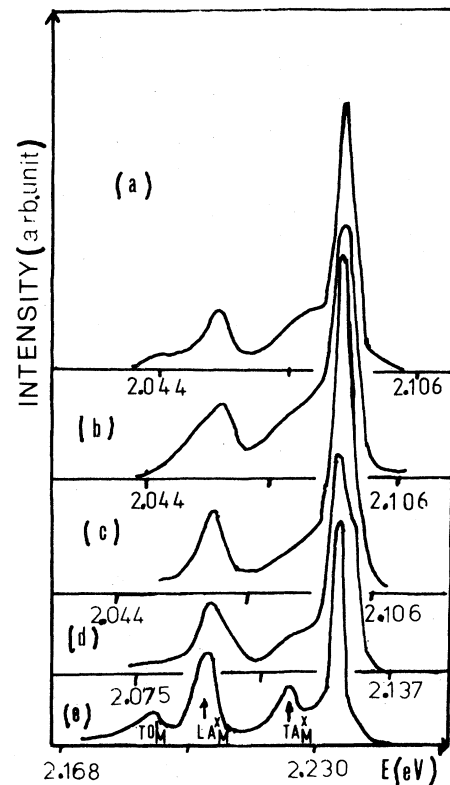


FIG. 1. Luminescence spectrum of $\text{GaAs}_{1-x}\text{P}_x$ at $T=2$ K and for excitation power $P=40$ mW/cm^2 : (a) $x=0.51$, (b) $x=0.52$, (c) $x=0.56$, (d) $x=0.61$, (e) $x=0.85$. $\text{TA}_M^x, \text{LA}_M^x$ are phonon replicas of M_0^x .

TABLE I. The energy of the LA_M^x -phonon replica observed for different compositions x .

	0.51	0.52	0.56	0.61	0.85
$E(LA_M^x)$ (meV)	30.5	30.6	30.8	30.8	31.2

The samples used for this study were grown by the metal-organic vapor-phase epitaxy (MOVPE) technique¹² and were nominally undoped. Residual impurities gave a net carrier concentration $n \leq 10^{16} \text{ cm}^{-3}$.

The luminescence spectra of $\text{GaAs}_{1-x}\text{P}_x$ for the compositions $x=0.51, 0.52, 0.56, 0.61, 0.85$ at $T=2 \text{ K}$ and for excitation power $P=40 \text{ mW/cm}^2$, are shown in Fig. 1. The M_0^x peak is assigned to the zero-phonon line due to carriers localized by the fluctuating potential. The LA_M^x -phonon replica of M_0^x is labeled M_1^x . The LA_M^x -phonon energies for different compositions x are shown in Table I. In addition to the LA_M^x -phonon replica we also observe TA_M^x - (13 meV) and TO_M^x - (47 meV) phonon replicas of M_0^x for the composition $x=0.85$ [Fig. 1(e)].

At higher excitation power density, the D_0^x and D_1^x peaks assigned, respectively, to the donor bound-exciton level and its LA_D^x -phonon replica are observed (Fig. 2). The relative intensities $I_{D_1^x}/I_{D_0^x}$ and $I_{M_1^x}/I_{M_0^x}$ are similar and hence seem not to depend on the degree of localization.

II. VARIATION WITH EXCITATION POWER DENSITIES

Figure 3 shows the intensity variations $I_{M_0^x}$ with excitation density P for the compositions $x=0.51, 0.52, 0.56, 0.61, 0.85$. The intensity variation is linear for small P ($P < 0.1 \text{ W/cm}^2$) and saturates already at $P \approx 1.0 \text{ W/cm}^2$. At saturation, the intensity $I_{M_0^x}$, which depends on the composition (Fig. 3), is the product of a density ρ and a probability for radiative recombination W . Here ρ

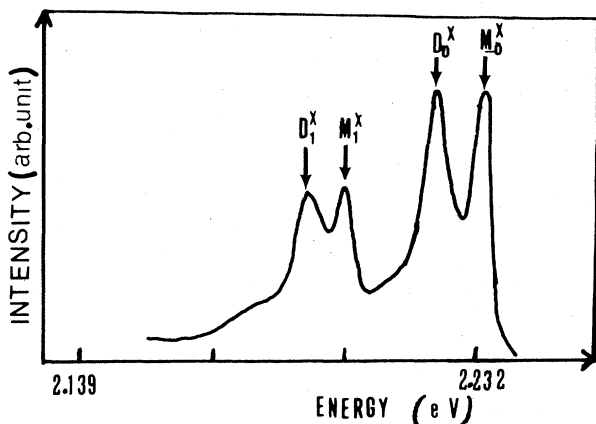


FIG. 2. Luminescence spectrum of $\text{GaAs}_{0.15}\text{P}_{0.85}$ at $T=5 \text{ K}$ and for excitation power $P=2.2 \text{ W/cm}^2$. M_1^x and D_1^x are LA^x -phonon replicas of M_0^x and D_0^x , respectively, (donor bound exciton).

is the total number of states in the localized tail below a mobility edge. The dependence of W on composition will be deduced later in Sec. IV from time-decay measurements.

Figure 4 shows the variation of $R(x)=I_{M_1^x}/I_{M_0^x}$ with composition x for different excitation power densities. $R(x)$ increases when x is increased from $x=0.5$ to 1.0 , and $R(x)$ depends strongly on the band-gap structure of the alloy, a so-called band-structure enhancement effect.¹⁰ Actually, for a sample with $x=0.49$ the M_1^x replica is very hard to even observe.

Figure 5 shows the different behavior with excitation power densities of the M_0^x , M_1^x , D_0^x , and D_1^x peak intensities. The variation is linear for D_0^x and for D_1^x in the whole excitation range, while there is a saturation at relatively low power densities ($P > 1.0 \text{ W/cm}^2$) for M_0^x and for M_1^x already observed in Fig. 3.

An important result from the data in Fig. 3 is that the M_0^x intensity clearly saturates and does *not* change from a linear to square-root dependence on power densities. This is in contradiction to the results reported by Lai and Klein,⁹ who interpreted such a change of the slope as being indicative of an Auger process of biexcitons. It is also worth noting that the saturation of M_0^x in our samples sets in for excitation power densities exceeding those observed by Lai and Klein^{8,9} by at least a factor of 10. The implication of this difference will be discussed below (Sec. VII).

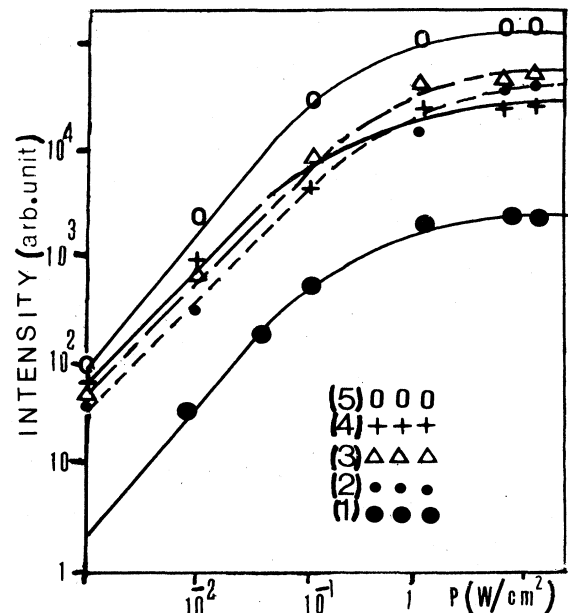


FIG. 3. Intensity of M_0^x as a function of excitation power P : (1) $x=0.85$, (2) $x=0.61$, (3) $x=0.52$, (4) $x=0.51$, (5) $x=0.56$.

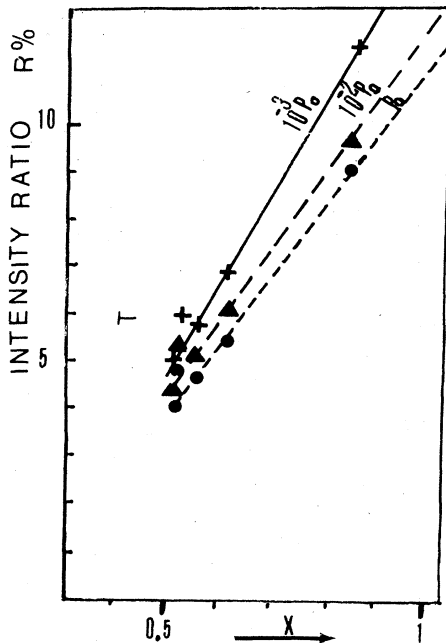


FIG. 4. Intensity ratio $R = I_{M_1^x} / I_{M_0^x}$ as a function of composition x , for different excitation powers: (a) $10^{-3}P_0$, (b) $10^{-2}P_0$, (c) $P_0 = 10 \text{ W/cm}^2$, in $\text{GaAs}_{1-x}\text{P}_x$ alloys.

III. THE LINE SHAPE OF M_0^x

As pointed out previously⁸⁻¹⁰ the M_0^x peak has an unusual, asymmetric shape (Fig. 6) with a sharp high-energy side. The energy of this high-energy cutoff may correspond to the separation of localized and delocalized states of particles responsible for the luminescence.¹⁰ The slope on the low-energy side has been suggested to reflect primarily the density of states in the tail region.

The result of careful measurements of the M_0^x line

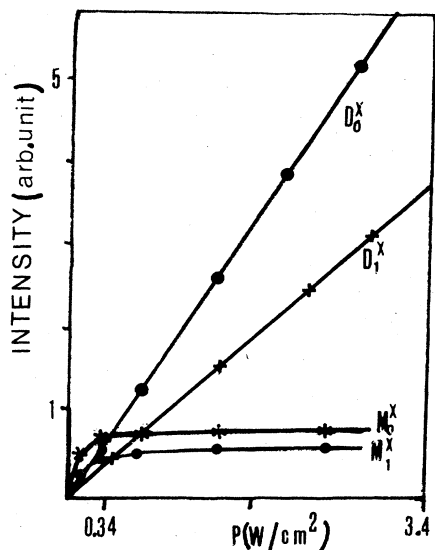


FIG. 5. M_0^x , M_1^x , D_0^x , and D_1^x intensities as a function of excitation power P , at $T = 5 \text{ K}$, $\text{GaAs}_{0.15}\text{P}_{0.85}$.

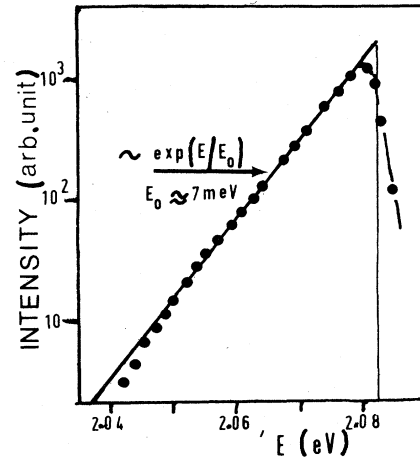


FIG. 6. Luminescence spectrum of M_0^x plotted semilogarithmically, displaying the exponential dependence of the low-energy tail.

shape, where resonant dye-laser excitation has been used, is shown in Fig. 6 for $x \approx 0.49$, a sample for which M_0^x dominates and D_0^x is not interfering for the excitation densities used. This semilogarithmic plot shows that the line shape of the low-energy side is well described by an exponential function, as expected for a density-of-states tail caused by a fluctuation potential. The slope of the fitted line gives $\rho(E) \propto e^{E/E_0}$ with $E_0 \approx 7 \text{ meV}$. This experimentally determined photon-energy dependence of the M_0^x line shape will later (Sec. VI) be used to calculate the temperature and delay-time dependence of the M_0^x line.

IV. TIME DEPENDENCE OF M_0^x

Detailed measurements of the luminescence decay for samples with different compositions x are presented in Figs. 7 and 8. The luminescence decay of M_0^x peak is nonexponential, and its lifetime ($\tau_{M_0^x} \approx 5-100 \mu\text{s}$) is considerably longer than the D_0^x exciton lifetime ($\tau_{D_0^x} \approx 200$

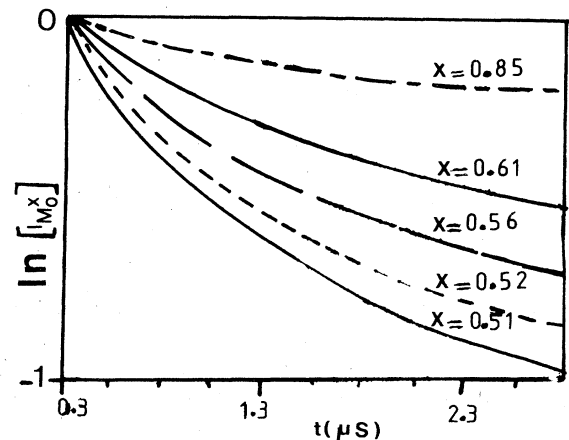


FIG. 7. Intensity time dependence of the M_0^x peak in $\text{GaAs}_{1-x}\text{P}_x$ alloys, at $T = 2 \text{ K}$ and for $P = 10 \text{ mW/cm}^2$.

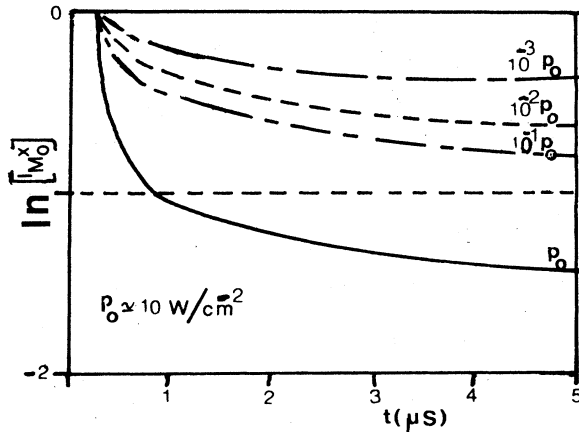


FIG. 8. Intensity time dependence of the M_0^x peak in $\text{GaAs}_{0.15}\text{P}_{0.85}$ at $T=2$ K and for different excitation powers; $P_0=10$ mW/cm^2 .

ns). Figure 7 shows that the luminescence decay of M_0^x becomes slower when the composition increases.

The dependence of luminescence decay with excitation power is shown in Fig. 8. The intensity decays more rapidly with increasing excitation power. At saturation, the $I_{M_0^x}$ decay is still nonexponential.

The time decay of a localized electron-hole pair in an indirect band-gap alloy has been treated by Klein *et al.*⁷ A nonexponential decay is found due to mixing of Γ states by the random potential. The distribution of decay rates was given as

$$P(W) = \langle W \rangle_{\text{av}}^{-1} \exp \left[-\frac{W}{\langle W \rangle_{\text{av}}} \right]. \quad (1)$$

$\langle W \rangle_{\text{av}}$ is the mean radiative decay rate without phonon assistance if the conduction-band minimum does not occur at the X point. $\langle W \rangle_{\text{av}}$ is a function of the degree of disorder in the alloy. The one-phonon radiative decay rate W_0 involving momentum-conserving phonons is independent of the degree of disorder, since it is not sensitive to mixing of Γ states.

We interpret Fig. 8 by considering that the faster decay of $I_{M_0^x}$ with decreasing composition x corresponds to an increase of $\langle W \rangle_{\text{av}}$ with decreasing energy difference $\Delta = E_g^\Gamma - E_g^x$. $\langle W \rangle_{\text{av}}$ also increases with increasing disorder, which is expected to be large in the middle-alloy range. As a consequence, the ratio $R = I_{M_1^x}/I_{M_0^x}$, which is proportional to $W_0/\langle W \rangle_{\text{av}}$, decreases with decreasing composition x and increases with decreasing power densities for a given composition (Fig. 4). We can understand the increasing R with decreasing power excitation by assuming that the population of states requiring a phonon to decay has a different intensity dependence than the states which can decay without phonon assistance. Those states which require phonon participation for their recombination decay slower and, hence, saturate for lower power densities.

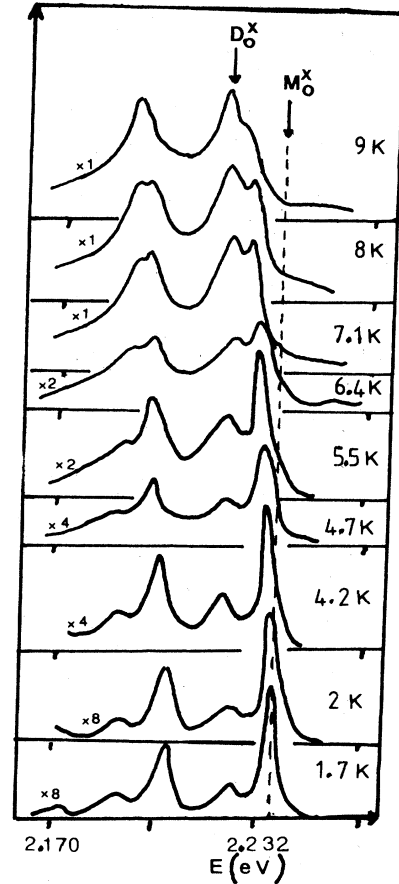


FIG. 9. Luminescence spectra of $\text{GaAs}_{0.15}\text{P}_{0.85}$ at different temperatures T , for $P=0.5$ W/cm^2 .

V. TEMPERATURE DEPENDENCE OF M_0^x

Figures 9 and 10 show the evolution of the luminescence spectra with temperature for $x=0.85$ and $x=0.51$, respectively. The M_0^x and M_1^x peaks shift to lower energies when the temperature increases from 2 to 8 K, but the D_0^x and D_1^x peak energies do not change. The shift is about 4.5 meV for $x=0.85$ and somewhat larger (about 6 meV) for $x=0.51$ due to overlap with D_0^x (Fig. 11). For $T > 10$ K, M_0^x and M_1^x peaks are not observed. D_0^x and D_1^x shift to lower energies much faster than the indirect band gap E_g^x when the temperature is varied from $T=10$ K to $T=23$ K. This shift of the D_0^x line might be due to thermal depopulation of the high-energy portion of the alloy-broadened D_0^x energy distribution. Estimates of the energy difference between the M_0^x line and the free-exciton energy (at low temperatures) give a scatter in the value of $\Delta(E_g^x - M_0^x)$ between 7 and 12 meV.

VI. MODEL AND CALCULATION OF TIME AND TEMPERATURE DEPENDENCE

In Sec. V it was shown that the M_0^x line varies strongly with temperature. Firstly, the energy position shifts approximately linearly with temperature with $dE/dT \approx 0.8$ meV/K. Secondly, the intensity of the peak is rapidly

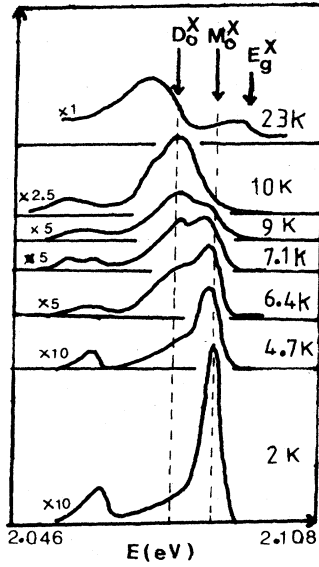


FIG. 10. Luminescence spectra of $\text{GaAs}_{0.49}\text{P}_{0.51}$ at different temperatures T , for $P=0.5 \text{ W/cm}^2$.

quenched even for very low temperatures, with an apparent activation energy of 2–4 meV.⁹ We will show here that by using the exponential line shape determined in Sec. III and a simple model, where the low-temperature, high-energy side of the peak is a mobility edge causing the quenching, we are able to generate the reported behavior of the M_0^x peak, including the variation of decay times

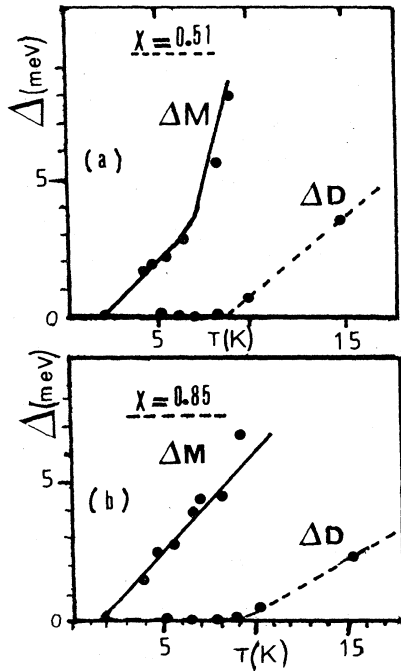


FIG. 11. Energy shift of M_0^x and D_0^x peaks as a function of temperatures T , in $\text{GaAs}_{1-x}\text{P}_x$. $\Delta M = E_{M_0^x}(T=1.7 \text{ K}) - E_{M_0^x}(T)$ and $\Delta D = E_{D_0^x}(T=1.7 \text{ K}) - E_{D_0^x}(T)$ shift. (a) $x=0.51$, (b) $x=0.85$.

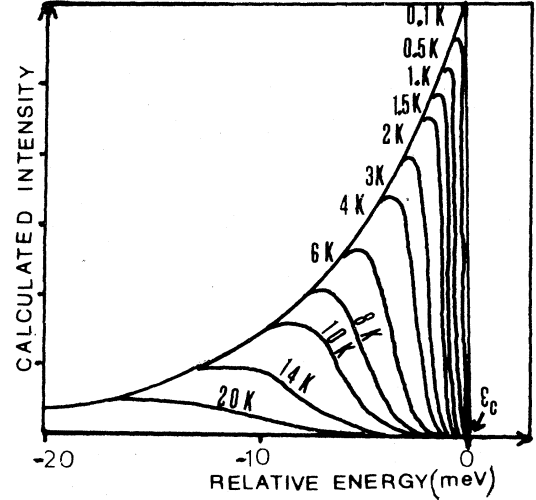


FIG. 12. The calculated line shape of M_0^x at different temperatures. E_c is the energy of the high-energy cutoff of M_0^x .

with emission photon energies.⁹ For the model calculations we assume that for each photon energy E in the peak the intensity can be written as

$$I(E, T, t) \propto \rho(E) \exp[-t/\tau_{\text{tot}}(E, T)] \frac{\tau_{\text{tot}}(E, T)}{\tau_{\text{rad}}}, \quad (2)$$

where $\rho(E)e^{-t/\tau_{\text{tot}}(E)}$ is the concentration of occupied states at energy E and time t and the last term is the radiative efficiency. We will for simplicity assume that the radiative recombination rate is independent of temperature T and energy E , which is a fairly good approximation although lower-lying states can be expected for more distant electron-hole pairs.

If we tentatively assume that the dominant nonradiative depopulation mechanism consists of thermal excitations from E to a critical E_c at which the excited particles become mobile and may recombine elsewhere, i.e., a mobility edge we can write

$$\begin{aligned} \tau_{\text{tot}} &= \left[\frac{1}{\tau_{\text{rad}}} + \frac{1}{\tau_{\text{nonrad}}} \right]^{-1} \\ &= \left[\frac{1}{\tau_{\text{rad}}} + \nu \exp\left[-\frac{E_c - E}{k_B T}\right] \right]^{-1}. \end{aligned} \quad (3)$$

As will be shown below we are able to identify the mobility edge E_c with the steep high-energy side of M_0^x observed for very low temperatures. τ_{rad} is experimentally determined and ν , an effective frequency for thermal excitation attempts, is the only fitting parameter. Figure 12 shows calculated M_0^x line spectra as functions of T , with a rapid shift to lower energies accompanying the thermal quenching. For $x \approx 0.5$ we have $\tau_{\text{rad}} \approx 20 \mu\text{s}$ and the frequency factor $\nu = 2 \times 10^8 \text{ s}^{-1}$ has been chosen to give agreement with the experimentally measured peak-position shift.

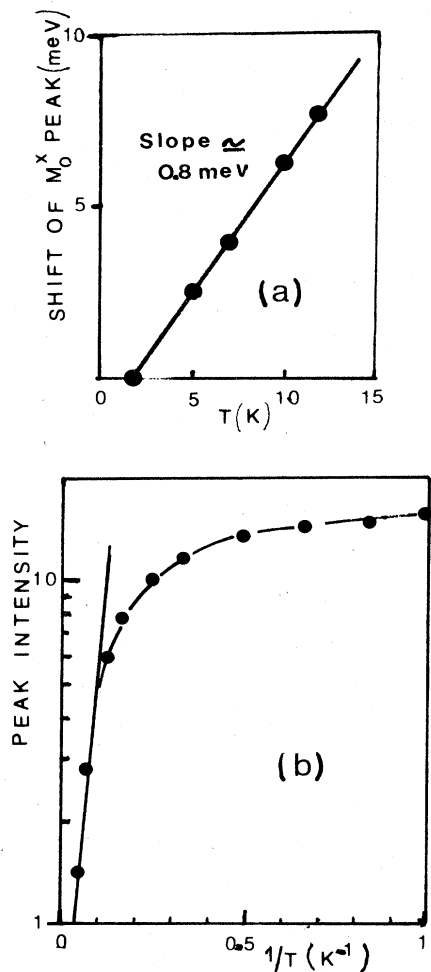


FIG. 13. (a) Calculated shift of the M_0^x peak as a function of temperature. (b) Calculated temperature quenching of the M_0^x line giving an apparent activation energy of 3 meV.

The peak position which has been plotted in Fig. 13(a) shifts *linearly* with increasing temperature, in agreement with experimental observations. The amplitudes calculated in Fig. 12 have been plotted semilogarithmically in Fig. 13(b) in order to determine an apparent activation energy for the thermal quenching for comparison with experimental estimates. Figure 13(b) gives an apparent activation energy of ~ 3 meV, in excellent agreement with published⁹ as well as with unpublished¹³ results.

The question, however, arises whether this agreement only can be found in a model where the quenching energy is identical to a mobility edge forming the low-temperature, high-energy side of the peak. Attempts to calculate spectra assuming that the thermal quenching occurs via higher lying states as has previously been suggested gives nonlinear shifts with temperature and higher activation energies, in disagreement with experiments.

The thermal quenching behavior should probably not be described by an exponential activation. As shown in Appendix A, the shift of the peak position as well as the peak intensity varies, for an exponential density-of-states

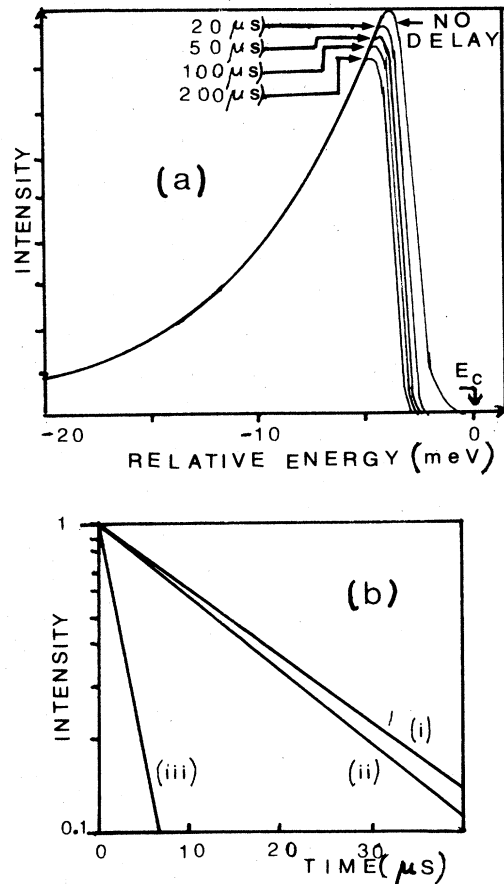


FIG. 14. (a) Calculated line shape of M_0^x at different delay times. The low-energy tail has been normalized to the same intensity in order to display the different decay times at different portions of the line. (b) Calculated intensity of (i) 1.4 meV towards the low-energy side from the peak, (ii) on the peak, and (iii) 1.4 meV towards the high-energy side from the peak plotted logarithmically versus time.

distribution, approximately linearly with T according to the model used [Eq. (2)].

It has been reported⁹ that the decay rate of the M_0^x line varies, depending on which portion of the line is studied. The parameters used in the calculated figures above have, with Eq. (2), been used to generate the time dependences shown in Fig. 14(a) and plotted for different positions around the peak in Fig. 14(b). The qualitative behavior is very similar to that experimentally found by Lai and Klein,⁹ lending further support to the model proposed.

VII. DISCUSSION

In this section we will collect the information that can be gained from the experimental data presented in Secs. I–V, from the model calculations in Sec. VI, and from the difference in the behavior of the samples studied here and samples investigated by other groups.

The saturation behavior displayed in Fig. 3 is qualitatively different from that reported previously,⁹ where only the onset of saturation was observed. The data in Fig. 3

therefore do not support the suggestion that the saturation is due to Auger recombination of biexcitons. Furthermore, the power density level at which saturation starts seems to depend strongly on the doping level of the samples. A comparison between the samples studied in this work and those previously investigated^{8,9} shows that our samples with 10 times lower donor doping levels saturate first at ~ 10 times higher power densities. We think that saturation depends on the density of states $\rho_{M_0^x}$, which can only recombine with the long lifetime, giving rise to the M_0^x luminescence. Since this luminescence recombination is very slow, we suggest that only those low-potential regions which do not contain any donors can contribute to the M_0^x luminescence. The concentration of states with long lifetimes should therefore be larger in our samples and saturation is then expected at higher power density levels. A rough estimate of the dependence on the donor concentration can be made, by noting that the possibility of not finding a donor, P , in a well of radius r is given by

$$P = \exp \left[-\frac{4\pi r^3 N_d}{3} \right]. \quad (4)$$

The observed differences gives

$$\frac{I_{M_0^x}(N_{d_1})}{I_{M_0^x}(N_{d_2})} = \exp \left[-\frac{4\pi r^3}{3} (N_{d_1} - N_{d_2}) \right], \quad (5)$$

which suggests an average radius $\langle r \rangle \sim 200 \text{ \AA}$, which would be a measure of the extent of the localized wave function.

The observation of this doping dependence of the M_0^x saturation suggests two possible interpretations of the high-energy edge of the M_0^x line. In one case (a) the edge is intrinsic in nature, a mobility edge, and the change in saturation conditions corresponds to a reduced effective M_0^x concentration equal to an increase in the concentration of potential wells with donors inhibiting the slow M_0^x recombination to be observed. In this case the position of the M_0^x line relative to E_q^x and D_0^x is independent of the donor concentration and the faster saturation corresponds to the lower number of M_0^x defects. In the other case (b) the high-energy edge corresponds to that energy for which the extension of the localized state has a high probability of overlapping with a donor. Since this critical extent must decrease with increasing donor concentration one would expect the critical energy to shift to lower energies (closer to the D_0^x peak) for increasing donor concentrations. However, in this case, the "active" M_0^x defects ought to become saturated at the same power level, independent of N_d .

Within experimental accuracy the energy position of M_0^x (relative to D_0^x) is identical in our samples and in those investigated by Lai and Klein. From all observations we therefore conclude that case a with a mobility edge of intrinsic nature seems to be the most likely origin

of the anomalous high-energy edge. It would, however, be very useful to study the M_0^x peak position at very low temperatures, for example, $< 1 \text{ K}$ (compare calculated results in Fig. 12), in comparable samples of varying N_d .

ACKNOWLEDGMENTS

We thank H. Mariette [Centre National de la Recherche Scientifique (CNRS) Bellevue-Meudon, France] for his experimental contribution of studying the variation of luminescence spectra with temperature and F. Mollot (Laboratoire de Physique des Solides de l'École Normale Supérieure, associé au CNRS, Université Paris VII, France) for use of equipment for taking time-resolved spectra. We also thank C. Benoit à la Guillaume for helpful discussions and comments on the manuscript.

APPENDIX A: ANALYTICAL SOLUTION FOR THE SHIFT OF THE PEAK POSITION WITH TEMPERATURE AND FOR THE THERMAL QUENCHING RATE

With the line shape given in Sec. VI for the M_0^x peak due to the recombination of disorder trapped carriers, we can solve for the energy position and for the amplitude of the peak, i.e.,

$$I(E) \propto \rho(E) \tau_{\text{tot}} \propto \exp(E/E_0) \left[\frac{1}{\tau_{\text{rad}}} + \nu \exp \left(\frac{E_c - E}{k_B T} \right) \right]^{-1}. \quad (A1)$$

$dI/dE = 0$ gives the approximate solution

$$E_{\text{max}} \approx E_c - k_B T \beta, \quad (A2)$$

where β is a function which varies slowly with temperature and can be evaluated for a typical temperature being investigated, T' :

$$\beta \approx \ln \left[\tau_{\text{rad}} \nu \frac{E_0}{k_B T'} \right]. \quad (A3)$$

Solving for the expected temperature dependence of the peak amplitude shows that the thermal activation energy that can be estimated from a plot of the logarithm of $I_{M_0^x}$ versus $1/T$ is only an approximation. A more careful treatment suggests that for a density of states which varies exponentially with energy, it is more relevant to plot the logarithm of $I_{M_0^x}$ versus T ,

$$\ln(I_{M_0^x}) \approx A - \frac{\beta k_B T}{E_0} \quad (A4)$$

with β defined as above [Eq. (A3)].

- ¹O. Goede, D. Hennig, and L. Johr, *Phys. Status Solidi B* **96**, 671 (1979).
- ²L. Samuelson, S. Nilsson, Z. G. Wang, and H. G. Grimmeiss, *Phys. Rev. Lett.* **53**, 1501 (1984).
- ³D. J. Wolford, B. G. Streetman, Shui Lai, and M. V. Klein, *Solid State Commun.* **32**, 51 (1981).
- ⁴S. Permogorov, A. Reznitskii, S. Verbin, G. O. Müller, R. Floegel, and M. Nikiforova, *Phys. Status Solidi B* **113**, 589 (1982).
- ⁵V. Agekeyan, R. Bindemann, R. Schwabe, Yu. Stepanav, and I. Streit, *Phys. Status Solidi B* **116**, K43 (1983).
- ⁶M. D. Sturge, E. Cohen, and R. A. Logan, *Phys. Rev. B* **27**, 2362 (1983).
- ⁷M. V. Klein, M. D. Sturge, and E. Cohen, *Phys. Rev. B* **25**, 4331 (1982).
- ⁸Shui Lai and M. V. Klein, *Phys. Rev. Lett.* **44**, 1087 (1980).
- ⁹Shui Lai and M. V. Klein, *Phys. Rev. B* **29**, 3217 (1984).
- ¹⁰L. Samuelson and M. E. Pistol, *Solid State Commun.* **52**, 789 (1984).
- ¹¹E. Cohen and M. D. Sturge, *Phys. Rev. B* **25**, 3828 (1982).
- ¹²L. Samuelson, P. Omling, H. Titze, and H. G. Grimmeiss, *J. Phys. (Paris) Colloq.* **12**, C5-323 (1982).
- ¹³M. Oueslati, Internal Report, Faculté des Sciences de Tunis (1983).